

# Differential Cross Section Measurement of $\eta$ Photoproduction on the Proton from Threshold to 1100 MeV

F. Renard<sup>1</sup>, M. Anghinolfi<sup>2</sup>, O. Bartalini<sup>3</sup>, V. Bellini<sup>4</sup>, J.P. Bocquet<sup>1</sup>, M. Capogni<sup>3,5</sup>, M. Castoldi<sup>2</sup>, P. Corvisiero<sup>2</sup>, A. D'Angelo<sup>3</sup>, J.-P. Didelez<sup>5</sup>, R. Di Salvo<sup>3,5</sup>, C. Gaulard<sup>6</sup>, G. Gervino<sup>7</sup>, F. Ghio<sup>8</sup>, B. Girolami<sup>8</sup>, M. Guidal<sup>5</sup>, E. Hourany<sup>5</sup>, V. Kouznetsov<sup>9</sup>, R. Kunne<sup>5</sup>, A. Lapik<sup>9</sup>, P. Levi Sandri<sup>6</sup>, A. Lleres<sup>1</sup>, D. Moricciani<sup>3</sup>, V. Nedorezov<sup>9</sup>, L. Nicoletti<sup>1</sup>, D. Rebreyend<sup>1</sup>, N. Rudnev<sup>10</sup>, M. Sanzone<sup>2</sup>, C. Schaerf<sup>3</sup>, M. L. Sperduto<sup>4</sup>, M.C. Sutura<sup>4</sup>, M. Taiuti<sup>2</sup>, A. Turlington<sup>11</sup>, Q. Zhao<sup>5</sup>, A. Zucchiatti<sup>2</sup>

(GRAAL collaboration)

<sup>1</sup> *IN2P3, Institut des Sciences Nucléaires, 38026 Grenoble, France*

<sup>2</sup> *INFN sezione di Genova and Università di Genova, 16146, Italy*

<sup>3</sup> *INFN sezione di Roma II and Università di Roma "Tor Vergata", 00133, Italy*

<sup>4</sup> *INFN sezione di Catania and Università di Catania, 95100, Italy*

<sup>5</sup> *IN2P3, Institut de Physique Nucléaire, 91406 Orsay, France*

<sup>6</sup> *INFN Laboratori Nazionali di Frascati, 00044, Italy*

<sup>7</sup> *INFN sezione di Torino and Università di Torino, 10125, Italy*

<sup>8</sup> *INFN sezione di Roma I and Istituto Superiore di Sanità, Roma, 00161, Italy*

<sup>9</sup> *Institute for Nuclear Research, 117312 Moscow, Russia*

<sup>10</sup> *Institute of Theoretical and Experimental Physics, 117259 Moscow, Russia*

<sup>11</sup> *RRC Kurchatov Institute, 123182 Moscow, Russia*

(December 4, 2000)

Measurement of the differential cross section for the reaction  $p(\gamma, \eta p)$  is presented from threshold to 1100 MeV photon laboratory energy. The experiment has been performed using the GRAAL facility in Grenoble. For the first time, the region of the  $S_{11}(1535)$  resonance is fully covered, allowing a precise extraction of its width. Above 900 MeV, s-wave dominance disappears while p and d-waves take over. A discussion about their origin is given, suggesting unexpected contribution from vector meson exchange or the need for "missing" resonances.

PACS numbers: 13.60.Le, 13.88.+e, 14.20.Gk, 25.20.Lj

The nucleon, as any composite object, shows a spectrum of excited states intimately connected to its internal structure. Precise measurements of the properties of these states offer a unique opportunity to test Quantum ChromoDynamics (QCD) in the non-perturbative regime and to approach the confinement problem. Historically, they have been first observed as baryon resonances in  $\pi$ -N scattering [1], giving a rich spectrum, typical of a few-body problem. Since the dominant decay channel of nucleon resonances is the strong decay through meson emission, photoproduction of light mesons ( $\pi$ ,  $\eta$ ,  $K$ ,...) provides a complementary way to access information about nucleon spectroscopy. Whereas elastic and inelastic  $\pi$ -N scattering have provided precise values for the masses and widths [2], meson photoproduction allows to measure the electromagnetic transitions, providing a stringent and dynamical test for models of the nucleon.

Among the large variety of existing models [3], Constituent Quark Models (CQM) have been the most successful in accounting for the observed spectrum. These "QCD-inspired" models describe the nucleon as three massive constituent quarks ( $m_Q \approx 300 \text{ MeV}/c^2$ ) confined by an harmonic potential. The hyperfine interaction, essential to reproduce the spectrum, is derived from gluon exchange in the original approach, or meson exchange in the more recent chiral version of CQM [1]. They also predict so far unobserved states ("missing resonances")

whose absence has been interpreted for instance by a weak coupling to  $\pi$ -N channels [4].

Extraction of resonances properties in pion photoproduction is a difficult exercise since one needs to disentangle many overlapping contributions [5,6]. By contrast, eta photoproduction close to threshold is strongly dominated by a single resonance, the  $S_{11}(1535)$ , and thus is the ideal place to investigate this benchmark state for nucleon models. Analyses of the available data base [7–10] have singled out two other resonances. On the one hand, the first quantitative extraction of the tiny  $D_{13}(1520)$  contribution could be achieved thanks to a rich set of data below 800 MeV ( $d\sigma/d\Omega$  [11], Target asymmetry [12]), including in particular our beam asymmetry  $\Sigma$  measurements between threshold and 1100 MeV [13]. Indeed, this resonance provides the main term in  $\Sigma$  through its interference with the  $S_{11}(1535)$ . On the other hand, to explain the unexpected large values of  $\Sigma$  above 1000 MeV and forward angles, the contribution of the  $F_{15}(1680)$  resonance has been proposed. To reach a definite answer however, complementary measurements are needed.

In this paper, we report on measurements of the differential cross section and extraction of the total cross section for the reaction  $p(\gamma, \eta p)$  from threshold  $E_\gamma = 707 \text{ MeV}$  ( $\sqrt{s} = 1485 \text{ MeV}$ ) to 1100 MeV ( $\sqrt{s} = 1716 \text{ MeV}$ ).

These data have been obtained with the GRAAL fa-

cility, located at the ESRF (European Synchrotron Radiation Facility) in Grenoble. The polarized and tagged photon beam is created by Compton backscattering of laser light on the 6.04 GeV electrons circulating in the storage ring. The measurements presented here used the green line ( $\lambda=514$  nm) of an Argon laser and the  $\gamma$ -ray energy spectrum extends from 500 MeV (geometrical limit of the tagging system) to the Compton edge at 1100 MeV. Detailed description of the beam,  $4\pi$  detector characteristics and acquisition system can be found in [13–16]. An energy deposition in the BGO calorimeter larger than 180 MeV in coincidence with an electron in the tagging system, triggers the data acquisition and allows to record simultaneously  $\pi^0 p$  and  $\eta p$  channels.

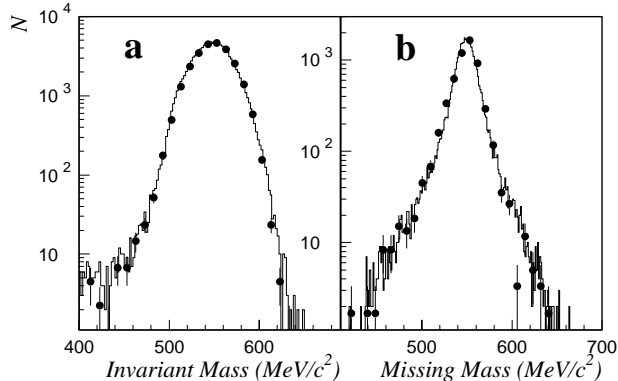


FIG. 1. a: Invariant mass spectrum for  $\eta \rightarrow 2\gamma$  decay. b: Missing mass spectrum, as calculated from the proton momentum. Data (full curve) and simulation (black dots) are presented with all other kinematical cuts applied.

Complete detection of the reaction products is requested in the event analysis. The photons from neutral  $\eta$  decays ( $\eta \rightarrow 2\gamma$  and  $\eta \rightarrow 3\pi^0 \rightarrow 6\gamma$ ) are identified in the BGO calorimeter, while the recoil proton is tracked in wire chambers and characterized by time of flight (ToF) and  $dE/dx$  measurements. With the tagger providing the energy of the incoming photon, the kinematics is overdetermined and a clean event selection is easily achieved using kinematical cuts (6 in total). Two examples are given with the invariant mass of the  $\eta$  (Fig. 1-a) and the missing mass calculated from the proton momentum (Fig. 1-b). For both quantities, the simulated spectrum nicely reproduces the experimental shape indicating the reliability of the simulation program and the absence of any electromagnetic background. The average hadronic background has been estimated to be less than 1% [16].

The cross section normalisation takes into account the target thickness, the photon beam intensity, the detection efficiency and the branching ratios of the  $\eta$ -meson decays taken from [2] ( $\eta \rightarrow 2\gamma$ :  $39.21 \pm 0.34$  %,  $\eta \rightarrow 3\pi^0$ :  $32.2 \pm 0.4$  %). The thickness of the liquid hydrogen target has been evaluated to  $0.217 \pm 0.003$  g $\cdot$ cm $^{-2}$  which gives a contribution of 1.5% to the systematic errors. Empty target runs have indicated a contribution of the target walls

of 0.9%, consistent with their thickness. The photon intensity is monitored by thin plastic scintillators located between the target and a total absorption calorimeter (Spacal) which serves as beam dump. Both detectors are in coincidence with the tagging system and their ToF spectra are measured for accidentals correction. The low efficiency of the thin monitor ( $\simeq 2.7\%$ ) prevents pile-up effects at high photon rate and is measured by comparison with the Spacal rate at low flux.

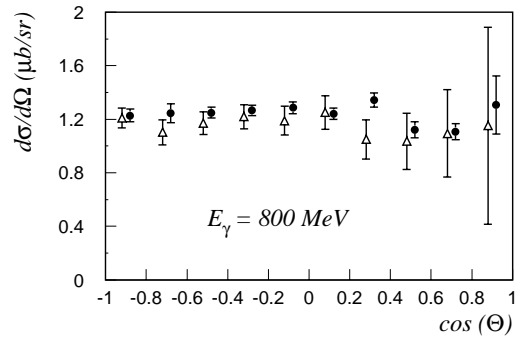


FIG. 2. Differential cross section for the  $p(\gamma, \eta p)$  reaction at 800 MeV. Results for events with  $\eta \rightarrow 2\gamma$  (black dot) and  $\eta \rightarrow 3\pi^0$  (open triangles) decays are compared.

The detector efficiency (50% on average) is calculated through the complete Monte-Carlo simulation of the apparatus, including the dependance of beam shape with energy and polarization, and using a realistic event generator [17]. Apart from the geometrical acceptance, the main loss comes from the overlap of clusters associated with  $\gamma$ -rays in the BGO ball (4 crystals hit on average per photon). This effect is strongly correlated to the  $\gamma$ -ray multiplicity as well as the cluster threshold and moreover is energy dependant. In order to test the reliability of our simulation code, the differential cross section has been calculated simultaneously for the two  $\eta$  decays:  $\eta \rightarrow 2\gamma$  and  $\eta \rightarrow 3\pi^0$ . The comparison at one energy (800 MeV) is displayed on Fig. 2 and illustrates the excellent agreement between both results. In addition, we have systematically used the high statistics reaction  $p(\gamma, \pi^0 p)$  to perform precise tests and comparisons with the world data base [16]. The error bars shown in the data correspond to the quadratic sum of all systematic and statistic errors except for those due to global normalisation factors estimated to be  $\pm 3.0\%$ .

The total cross section has been obtained by integration of the differential cross section, using a polynomial fit in  $\cos \theta$  to extrapolate the unmeasured region ( $\simeq 10\%$ ). A good reduced  $\chi^2$  is already achieved with a polynomial of degree two in agreement with the smooth behaviour observed in our measurements. However, this result depends on the extrapolation procedure which is a source of error that cannot be evaluated experimentally.

The total cross section calculated from threshold to 1100 MeV is plotted in Fig. 3. One can notice the

nice agreement with previous measurements obtained at Mainz [11] and Bonn (electroproduction at low  $Q^2$ ) [18] except a small discrepancy around 800 MeV.

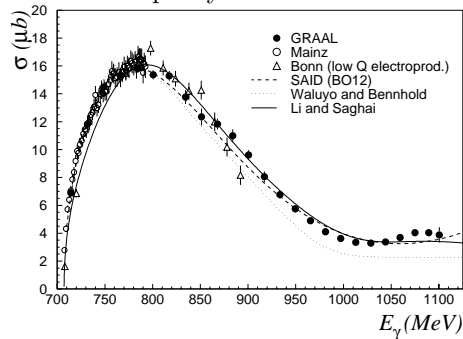


FIG. 3. Total cross section of the  $p(\gamma, \eta p)$  reaction. The GRAAL results (close circles) are compared to previous experimental results and to three different analyses. See text for details.

As mentioned earlier, the  $S_{11}(1535)$  resonance strongly dominates  $\eta$  photoproduction up to 900 MeV and its parameters (mass, width, helicity amplitude and decay branching ratio) can be directly estimated from the shape of the total cross section. Using data from Mainz and Bonn, the authors of ref. [19] have performed a comprehensive study to investigate these parameters. They showed that a considerable reduction of the uncertainties reported by the Review of Particle Physics could be achieved but also underlined some inconsistency with their estimates in particular about the extracted width. Whereas the Review quotes  $\Gamma_R \approx 150$  MeV (based only on  $\pi$ -N scattering data [2]), they obtained values close or larger than 200 MeV whatever the condition they explored. Since our measurement now fully covers the resonance, we can help clarify this issue. Performing a Breit-Wigner fit for the combined sets of data (GRAAL, Mainz), limited to energies less than 950 MeV, we found  $\Gamma_R = 170 \pm 20$  MeV, value which is now in agreement with  $\pi$ -N analyses and also with a recent electroproduction experiment at JLab [20]. The other resonance parameters can also be obtained, however the present reaction alone cannot constrain them simultaneously. In view of a precise and reliable extraction of the  $S_{11}(1535)$  parameters, one now needs a global analysis of the full set of data including  $(\gamma, \eta)$  as well as  $(\pi, \pi)$  and  $(\pi, \eta)$  results. Moreover, small additional contributions are also a source of uncertainties and have to be identified first.

The differential cross section, plotted in Fig. 4 for a sample of photon energies as a function of  $\cos \theta$  where  $\theta$  is the  $\eta$  C.M. polar angle, has been measured every 17 MeV between threshold and 1100 MeV (233 points). For the two lower energies of the figure, data from Mainz are also shown and illustrate the good agreement between both experiments. Thanks to the overwhelming dominance of the  $S_{11}(1535)$  resonance, the differential cross section can be expanded in terms of the s-wave multipole and its

interferences with other multipoles. Limiting the expansion to p and d waves, approximation valid at least up to 900 MeV, the following expression can be derived [9]:

$$\frac{d\sigma}{d\Omega} = \frac{q_\eta}{k} \{a + b \cos \theta + c \cos^2 \theta\} \quad (1)$$

where,  $q_\eta$  and  $k$  are the  $\eta$  and  $\gamma$  C.M. momenta, and

$$\begin{aligned} a &= |E_{0+}|^2 - \text{Re}[E_{0+}^*(E_{2-} - 3M_{2-})] \\ b &= 2 \text{Re}[E_{0+}^*(3E_{1+} + M_{1+} - M_{1-})] \\ c &= 3 \text{Re}[E_{0+}^*(E_{2-} - 3M_{2-})] \end{aligned}$$

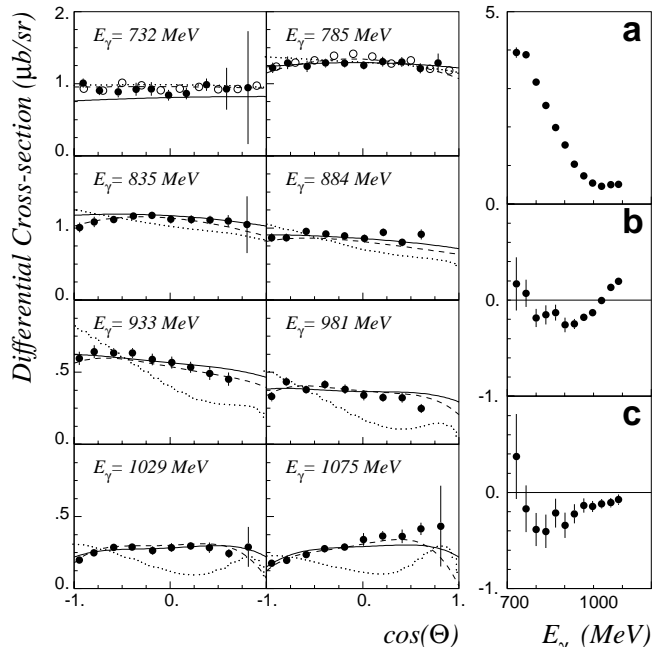


FIG. 4. Differential cross section for the  $p(\gamma, \eta p)$  reaction. Legend as in Fig. 3. The coefficients  $a$ ,  $b$  and  $c$  result from the fit to the data by expression (1).

In accordance with these simple expressions, contributions from p and d-waves will appear in the  $b$  and  $c$  coefficients respectively. We have fitted our results with expression (1) and the extracted coefficients are plotted versus  $\gamma$ -ray energy on the right-hand side of Fig. 4. As expected, the  $D_{13}(1520)$  contribution already seen in ref. [11] close to threshold is observed in  $c$ . More interesting, the significant  $b$  values above 800 MeV indicate a p-wave contribution not seen before. Above 1000 MeV, s-wave dominance breaks down and a simple interpretation of the sizeable values of these two coefficients is no longer possible. To get a more quantitative picture, we present now three analyses that take into account not only the cross section but also  $\Sigma$  results previously measured.

A multipole analysis, including our data, has been performed by the GWU group [21]. They achieved a nice global fit of the cross section (dashed line, Fig. 3 and 4) and equally of  $\Sigma$  (Fig. 5), for which we have displayed the highest energy published in 1998 and a new measurement using a UV laser line, confirming the large values at forward angle. Only s, p and d multipoles are

needed which rules out a strong contribution from the  $F_{15}(1680)$ . Analysis of the individual multipoles confirms the previous qualitative conclusions and indicates above 900 MeV the dominance of p and d-waves amplitudes. These higher multipoles can be associated to nucleon resonances ( $P_{11}(1710)$  or  $P_{13}(1720)$  for instance), but additional contributions can originate from vector meson exchange as well as nucleon Born terms. The two models discussed hereafter bring different answers.

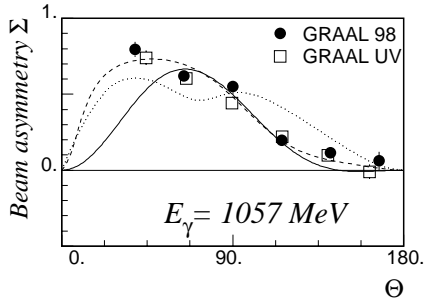


FIG. 5. Beam asymmetry  $\Sigma$  for the  $p(\gamma, \eta p)$  reaction. Results published in 1998 (circles) are compared to new results obtained with a UV line (squares). Legend as in Fig. 3

The first one from Waluyo and Bennhold [22,23] is a coupled-channel calculation based on the Bethe-Salpeter equation in the K-matrix approximation. It includes all hadronic and electromagnetic reactions with  $\gamma N$ ,  $\pi N$ ,  $\pi\pi N$ ,  $\eta N$ ,  $K\Lambda$ ,  $K\Sigma$  and  $\eta' N$  asymptotic states. Nucleon resonances with spin  $J \leq 3/2$  are included up to  $M = 2$  GeV. The results, based on a large data base, are plotted on Fig. 3 to 5 (dotted line), showing a fair overall agreement especially for  $\Sigma$  and to a less extent for  $d\sigma/d\Omega$ , in particular at high energy. Their unexpected conclusion is that above 900 MeV, the forward peaking of  $\Sigma$  is primarily due to intermediate vector meson exchange in the t-channel.

The second one from Li and Saghai [7,24] is based on a quark model, including therefore all known resonances. To avoid double counting, vector meson exchange in the t-channel is excluded, approximation valid as long as resonant contributions dominate. An interesting property of this approach is that it links directly data to the quark model, hence to quantities such as mixing angles of resonance configurations [25]. The model, constrained by our data only, is able to reproduce quite well the global trend for the cross section as well as for  $\Sigma$  (full curve). Looking in more details, significant deviations are nonetheless observed in the cross section near threshold and above 1000 MeV, and also in  $\Sigma$  at forward angle. The  $F_{15}(1680)$  plays a role but only through interference with other resonances and does not explain the forward peaking of  $\Sigma$ , consistently with the two previous studies. To improve on the model, the authors are currently working on the exciting possibility to add "missing" resonances.

In summary, we have measured the differential cross section for the reaction  $p(\gamma, \eta p)$  from threshold to 1100 MeV photon lab energy, completing our previous

measurement of the beam asymmetry  $\Sigma$  over the same energy range. Below 900 MeV, the reaction mechanism is well understood and these data will contribute to a precise determination of the dominant  $S_{11}(1535)$  parameters. Above this energy, data show a rapid transition to a completely different picture, that two models based on different approaches are not able to reproduce satisfactorily. Preliminary conclusions of their respective analyses suggest : an important and unexpected vector meson exchange contribution for the first one; the need for additional ("missing" ?) resonances for the second. They nevertheless agree with a multipole analysis to rule out the  $F_{15}(1680)$  as the source of the forward peaking of  $\Sigma$ .

We are grateful to C. Bennhold, B. Saghai and I. Strakovsky for helpful discussions and communication of their analyses prior to publication. It is a pleasure to thank the ESRF for a reliable and stable operation of the storage ring and the technical staff of the contributing institutions for essential help in the realization and maintenance of the apparatus.

\* Electronic address: rebreyend@isn.in2p3.fr

- [1] For a recent review, see T.P. Vrana, S.A. Dytman, T.S.H. Lee, Phys. Rep. **328** (2000) and references therein.
- [2] Review of Part. Phys., Eur. Phys. J. **C15**, 1-878 (2000).
- [3] Models of the nucleon, R.K. Bhaduri (Addison Wesley, 1988).
- [4] S. Capstick and W. Roberts, Phys. Rev. **D47**, 1994 (1993); Phys. Rev. **D49**, 4570 (1994).
- [5] R.A. Arndt, I.I. Strakovsky and R.L. Workman, Phys. Rev. **C56**, 577 (1997).
- [6] D. Drechsel, O. Hanstein, S.S. Kamalov and L. Tiator, Nucl. Phys. **A645**, 145 (1999).
- [7] Z. Li and B. Saghai, Nucl. Phys. **A644**, 345 (1998).
- [8] N. Mukhopahyay and N. Mathur, Phys. Lett. **B444**, 7 (1998).
- [9] L. Tiator, D. Drechsel, G. Knochlein, C. Bennhold, Phys. Rev. **C60**, 035210 (1999).
- [10] R. Workman, R.A. Arndt, I. Strakovsky, Phys. Rev. **C62**, 048201 (2000).
- [11] B. Krusche *et al.*, Phys. Rev. Lett. **74**, 3736 (1995).
- [12] A. Bock *et al.*, Phys. Rev. Lett. **81**, 534 (1998).
- [13] J. Ajaka *et al.*, Phys. Rev. Lett. **81**, 1797 (1998).
- [14] P. Levi Sandri *et al.*, Nucl. Inst. Met. **A370**, 396 (1996).
- [15] D. Barancourt *et al.*, Nucl. Inst. Met. **A388**, 226 (1997).
- [16] F. Renard, Thesis Univ. J. Fourier (Grenoble, 1999), available upon request.
- [17] L. Mazzaschi *et al.*, Nucl. Inst. Met. **A436**, 441 (1994).
- [18] M. Wilhelm, Ph.D. thesis, Univ. of Bonn, unpublished; B. Schoch, Prog. Part. Nucl. Phys. **34**, 43 (1995).
- [19] B. Krusche *et al.*, Phys. Lett. **B397**, 171 (1997).
- [20] C.S. Armstrong *et al.*, Phys. Rev. **D60**, 052004 (1999).
- [21] R.A. Arndt, I.I. Strakovsky and R.L. Workman, BAPS **45**, 43 (2000) and Private communication.
- [22] A. Waluyo and C. Bennhold, Private communication.
- [23] C. Bennhold *et al.*, nucl-th/9901066, nucl-th/0008024, T. Feuster and U. Mosel, Phys. Rev. **C59**, 460 (1999).
- [24] B. Saghai, Private communication.
- [25] B. Saghai, N\*2000 Workshop Proceedings (to appear in World Scientific), JLab (2000).